

Experimental study of a modified evaporative photovoltaic chimney including water sliding

M. Lucas^{a,*}, J. Ruiz^a, F.J. Aguilar^a, C.G. Cutillas^a, A.S. Kaiser^b, P.G. Vicente^a

^a Departamento de Ingeniería Mecánica y Energía, Universidad Miguel Hernández, Avda. de La Universidad, s/n, 03202, Elche, Spain

^b Departamento de Ingeniería Térmica y de Fluidos, Universidad Politécnica de Cartagena, Dr. Fleming, s/n, 30202, Cartagena, Spain

ARTICLE INFO

Article history:

Received 2 July 2018

Received in revised form

21 September 2018

Accepted 3 November 2018

Available online 12 November 2018

Keywords:

Solar cooling

Solar chimney

Evaporative cooling

PV/T

Cooling tower

HVAC

ABSTRACT

Solar cooling provides an ideal coupling between solar energy and the need for cooling, since both reach their maximum during the summer. However, solar refrigeration technologies either have not been competitive or are in a preliminary stage of development. Photovoltaic (PV) driven compression chillers are the most promising and close to market solar solutions today in the case of small to medium units (≈ 50 kW cooling) due to the tremendous decrease in the cost of PV modules. The main objective of this work is to improve the efficiency of a PV panel by cooling it on its upper face by water sliding and on its back side using a solar chimney. In addition, the system is used as heat sink of a water chiller working as a low scale cooling tower. The work developed consisted of adapting and testing a prototype, changing its mode of operation to overcome the limitations encountered in the first campaign of measures. Several tests were performed by modifying the water mass flow rate circulated to the nozzles (spray) and onto the PV upper surface (water film). For the test with a water flow rate in nozzles of 500 l/h and sliding 250 l/h the results show an average cooling of the panel of 15°C and an improvement in the electrical efficiency of the panel of about 10%. The modified system is still able to dissipate a thermal power of about 1500 W with a thermal efficiency exceeding 30% in summer conditions.

© 2018 Elsevier Ltd. All rights reserved.

1. Introduction

The air conditioning of buildings means 50% of the final energy demanded in the European Union, [3]. An increase in the coming years due to the increase of the ambient temperature and the greater exigencies of comfort can be predicted. This increase in the energy consumption of HVAC equipment will be associated with higher CO₂ emissions into the atmosphere unless alternative solutions to existing ones are proposed. Solar cooling is an attractive idea because of the chronological coincidence between available radiation and cooling needs. The challenge is to design an efficient and competitive solar air conditioning system. To date, different technical solutions have been studied combining solar energy and air conditioning. However, these technologies either have not been competitive or are still at a preliminary stage of development, [12].

Solar energy can be used for air conditioning in two ways mainly. On the one hand are the thermal systems of air conditioning where the solar irradiance is converted into refrigeration by

the use of thermal solar collectors and absorption or adsorption schemes. On the other hand, it is possible to use photovoltaic air conditioning systems. In this second option the electricity generated by the photovoltaic panels can be used for the drive of the compressor of a conventional equipment of air conditioning by steam compression.

Solar thermal air conditioning has difficulty emerging as a competitive solution for technical reasons such as the need to install large hydraulic systems, the complexity in the management of solar resources and risk management due to overheating between the two seasons (summer-winter). In addition, absorption technology generally uses and needs cooling towers that consume water, chemical treatments and faces the risk of developing Legionella. But above all, there are economic reasons. The cost of investing in solar refrigeration continues to be relatively high (3 or 5 times greater than a reversible heat pump), especially for small systems.

On the other hand, photovoltaic-based vapor compression systems are the most promising systems for medium and low power (≈ 50 kW) according to the International Energy Agency, [11]. To date, it appeared that solar air-conditioning systems were more

* Corresponding author.

E-mail address: mlucas@umh.es (M. Lucas).

Nomenclature			
A_V	Surface area of the water droplets (m^2/m^3)	β_{ref}	Temperature coefficient of η_{PV} ($1/^\circ\text{C}$)
C_p	Specific heat capacity ($\text{J}/(\text{kg K})$)	γ	Temperature coefficient of P_{max} ($\%/^\circ\text{C}$)
G_T	Irradiance (W/m^2)	η_{PV}	Electrical efficiency
h	Specific enthalpy of moist air (J/kg_a)	η_T	Thermal efficiency
h_D	Mass transfer coefficient ($\text{kg}/(\text{s m}^2)$)	<i>Subscripts</i>	
$h_{f,w}$	Specific enthalpy of saturated water liquid at T_w (J/kg_w)	1	Water inlet
$h_{s,w}$	Specific enthalpy of saturated water vapor at T_w (J/kg_w)	2	Water outlet
I_{mpp}	Nominal current (A)	a	Air
I_{sc}	Short circuit current (A)	amb	Ambient
k	Ross coefficient ($\text{K m}_2/\text{W}$)	cond	Condenser
m	Mass flow (kg/s)	i	Air inlet
N	Number of cells	int	Air intermediate
P_{mpp}	Module maximum power (W)	out	Air outlet
\dot{Q}	Cooling power (W)	w	Water
T	Temperature ($^\circ\text{C}$)	wb	Wet bulb
V_{oc}	Open circuit voltage (V)	<i>Abbreviations</i>	
V_T	Evaporative cooling volume (m^3)	BIPV	Building integrated photovoltaics
<i>Greek symbols</i>		NTU	Number of transfer units
α	Temperature coefficient of I_{sc} ($\%/^\circ\text{C}$)	PV-C	Photovoltaic driven cooling
β	Temperature coefficient of V_{oc} ($\%/^\circ\text{C}$)	PV	Photovoltaic cell
		PV/T	Photovoltaic thermal hybrid solar system
		RES	Renewable energy source
		ST-C	Solar thermal driven cooling

likely to be integrated in the case of large buildings since only solar thermal systems were used. However, the situation has changed with the enormous development of the domestic and commercial air conditioning equipment of medium power, as well as the tremendous decrease of the cost of the of the photovoltaic panels. Over the past years a very intense work has being done in this field [4], but we are still far away from what is achievable.

One of the major problems which is currently limiting the state-of-the-art solar cooling is related to the efficient conversion of solar energy to electricity. The efficiency of photovoltaic systems depends highly on the cell temperature. The PV module heating reduces its efficiency dramatically, [16]. The open-circuit voltage decreases significantly with the increase of PV module temperature ($-0.45\%/^\circ\text{C}$ for crystalline silicon), while the short cell circuit current increases only between 0.04 and 0.09 $\%/^\circ\text{C}$ (for crystalline silicon). So, these two effects together reduce the maximum available power (and consequently the electrical efficiency) between -0.3 and $-0.5\%/^\circ\text{C}$, [10].

Different techniques for reducing PV modules temperature using cooling systems have been found in the literature. Some of them work by passing air or water on the rear surface through channels or ducts, using natural convection or forced convection by a fan, [7,17]. The cell temperature of these PV modules is very much influenced by the capability of ventilating this channel. In other studies the PV module is cooled by spraying water on the top surface of the module. This method was used and the results showed an increase in output power in the range of 4–10%, [14]. The module temperature dropped significantly to about 20% leading to an increase in the PV module efficiency by 9% with active water cooling, by incorporating a heat exchanger at the rear surface of the module, [1]. Sometimes, extracted thermal energy can then be used for heating purposes such as producing domestic hot water in photovoltaic–thermal (PV/T) systems. Reddy et al. [15] reviewed recent advances in hybrid solar photovoltaic/thermal (PV/T) systems. However, no design has been found in the literature that combines the cooling of the photovoltaic module with

condensation of an air conditioning system as the system proposed in this paper.

The second key component of a PV driven compression chiller is the refrigeration equipment. Again, the operating temperature becomes the main variable in determining the performance of the equipment. Commercially, mainly air or water condensed chillers are used. Cooling systems that use water for condensation operate at lower condensing temperatures. This way, the energy consumption of these systems compared with the air condensed systems is lower. The effect of decreasing the condensing temperature on the power absorbed by the compressor can be from 1.8 to 4% per degree Celsius [18], depending on the cycle under consideration and the refrigerant used. The best energy efficiency of water-condensed systems is associated with the decrease in CO_2 emissions to the atmosphere. Water-condensed cooling systems usually work with cooling towers or evaporative condensers. Evaporative cooling systems are based on the evaporation of water inside a space, producing lower temperature and higher humidity. The change from liquid to vapor requires energy, which is extracted from the air by cooling it and increasing its humidity. This brings about a change from sensitive heat (drop in temperature) to latent heat (increase in water content in the mix of humid air).

The objectives of the patented Photovoltaic Evaporative Chimney [9] are twofold, (see Fig. 1). On the one hand, the system seeks to cool the photovoltaic module and, on the other, to dissipate heat from a refrigeration cycle. To this end, the solar chimney is divided into two main parts. Following the path of the airflow; the first section, called the evaporative cooling zone, has a series of nozzles that spray water parallel to the downward airflow. In this section the heat and mass transfer between water and air occurs. As the water descends, a small part evaporates, cooling the remaining water. This zone works as a small scale cooling tower. The air that has been in contact with water and may have reduced its temperature (it will depend on ambient conditions) then rises up due to buoyancy force through the second part, called the convective zone. Therefore, the second section is basically a solar chimney. The

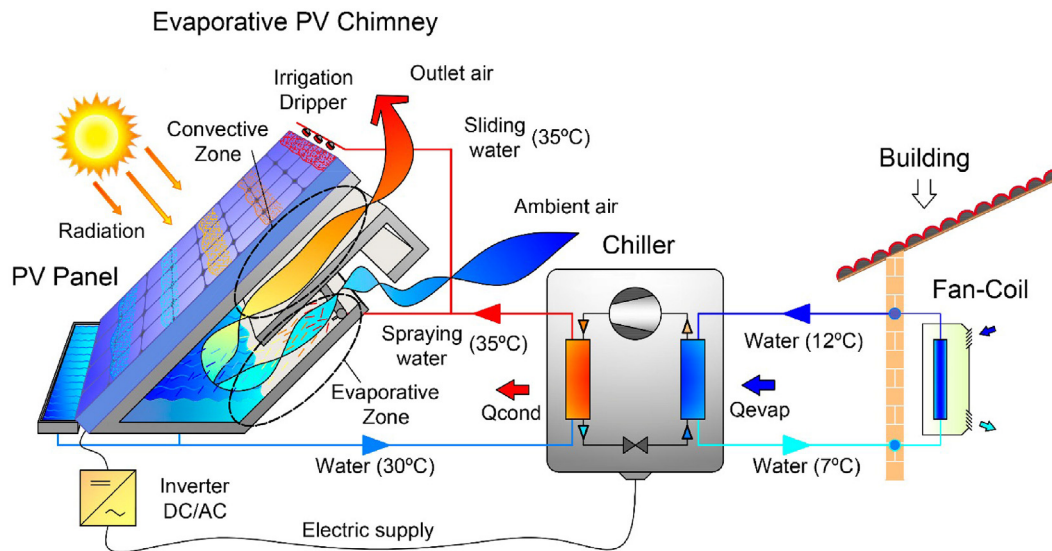


Fig. 1. Evaporative PV Solar Chimney and Air conditioning system scheme proposed. Numerical values are included in the drawing for reference only and to facilitate the reader's understanding.

photovoltaic module is cooled by the air stream flowing through the rear and, consequently, an improved performance can be obtained. The working hypothesis for this paper is based on improving the efficiency of photovoltaic modules using evaporative cooling. The water used for cooling the modules will be available to be used for the condensation of a refrigeration cycle.

It is necessary to point out, as background to this work, that in the summer of 2015 a first version of the prototype was designed, constructed and studied experimentally, [8]. The system was able to dissipate a thermal power of about 1500 W with a thermal efficiency exceeding 30% in summer conditions. The module temperature differences reached 8 °C, depending on the wind conditions and ambient air psychrometric properties. Regarding the electrical efficiency, the results showed an average improvement of 4.93% to a maximum of 7.66% around midday in a typical summer day for a Mediterranean climate. However, after this first campaign of measurements, we detected some aspects to improve. On the one hand, it was detected that, although the panel could be cooled and thus improve the performance of the PV panel, the temperature of the panel was not uniform, which was greater as the air rose inside the solar chimney. On the other hand, it was also verified that in high wind conditions (≈ 2.5 m/s) the improvement of the proposed design disappears even being detrimental since the level of wind was superior to the convective current induced inside the chimney. These results led to the modification of the prototype design. The objective of the present work is the modification of the evaporative photovoltaic chimney by adding a water slide system on the upper face of the photovoltaic panel and its experimental study.

2. Method

2.1. Experimental setup

The Photovoltaic Evaporative Chimney prototype was installed on a laboratory roof at the Universidad Miguel Hernández (38°16'N), Spain. The basis of the solar installation consists of two photovoltaic modules Sunrise, SR-P660255, see specifications on Table 1, arranged as shown in Fig. 2. The module located on the right was used as a reference (Module 1) and the module on the left was modified on the back side including the evaporative solar

Table 1
Specifications Sunrise module SR-P660255.

Magnitude	Units	Value
Maximum Power, P_{mmp}	W	255
Tolerance p_{mmp}	%	0/+3
Dimensions	mm	1637 × 992 × 40
Number of cells, N		60
Cell Type	156 × 156 mm	Poly-Crystalline Silicon
Module Efficiency	%	15.7
Short Circuit Current, I_{sc}	A	9.11
Open Circuit Voltage, V_{oc}	V	37.49
Nominal Current I_{mpp}	A	8.44
Nominal Voltage V_{mpp}	V	30.24
Temp. Coeff. of I_{sc} , α	(%/°C)	0.55
Temp. Coeff. of V_{oc} , β	(%/°C)	-0.33
Temp. Coeff. of P_{mmp} , γ	(%/°C)	-0.44



Fig. 2. Prototype of Photovoltaic Evaporative Chimney modified including sliding water system.

chimney (Module 2). The orientation for the PV modules is true south (Azimuth angle 0°) and tilt angle is fixed at 45°. In addition,

the laboratory building is a freestanding building, so the prototype will not be affected by shadows of other construction elements or facilities except late in the afternoon.

Both PV modules were directly connected to a micro-inverter equipment to convert the direct current produced by the PV modules (24 V) into alternate current (230 V). A grid-tied micro-inverter (APsystems YC500A) with intelligent networking and monitoring systems to ensure maximum efficiency, with a nominal power of 500 W, and independent electrical connection to the modules was used. This equipment was selected because it had an independent maximum power point control for each module, in addition of being perfectly adjusted to the technical characteristics of the PV facility. To dissipate the energy produced by the PV modules, an electrical load of 750 W was installed. An electrical inhibitor was connected between the electrical production point and the consumption point, to avoid injecting the electrical energy produced by the PV modules into the grid. Thus, the whole energy produced was self-consumed by the facility. This inhibitor consisted of an Arduino microcontroller capable of processing the information from a clamp ammeter installed on the main wire and adapting the energy consumption by using the electrical resistance in order to avoid the energy injection into the grid.

The hydraulic circuit is composed of a network of PVC pipes, see Fig. 3. A pump (ESPA Mod. Prisma 15 3 M), recirculates water from the tank to the nozzles arranged linearly in the input section of the solar chimney. The flat spray nozzles (Spraying Systems Co. Mod. ProMax Clip-Eyelet spray angle 110°) atomize the water evenly. The sprayed water mass flow rate can be changed manually by means of a balancing valve (STAD DN15). An electrical heater (1.5 kW) immersed in the tank is used to simulate the thermal load of the air conditioning machine. A water float ball valve is used to automatically fill the tank and also a filter is included to eliminate all kinds of things that can be harmful entering the pump.

The most notable change in the prototype design is the inclusion of the sliding water system. Water is distributed using 12 adjustable water irrigation drippers (0–80 l/h), which are installed at the upper side of Module 2. Water is then collected at the lower part of the PV modules via a drain channel, returning back to the water tank. The total water mass flowrate circulated to the solar chimney can be changed manually by means of a balancing valve.

To experimentally analyze the thermal and electrical

performance of the Photovoltaic Evaporative Chimney a series of variables were monitored and recorded. The first group of sensors are responsible for measuring environmental conditions: ambient air temperature, air relative humidity, wind speed and wind direction all of them are measured with a meteorological station placed on our laboratory roof just beside the experimental facility. A first class pyranometer installed in the same plane of the PV modules is used to measure radiation. The variables related to the thermal performance of the system are: air temperature and relative humidity measured at the transition point between the evaporating section and the convective section and at the output section, air velocity inside the solar chimney, inlet and outlet water temperatures, water mass flow and water consumption. Nine K-type thermocouples were installed on the rear side of each module distributed in a matrix form to measure the temperature of the PV modules. Regarding electrical parameters, voltages of each are directly measured and the currents of each module are determined from a value of voltage drop produced in a shunt resistor, calibrated to the passage of electric current. A general-purpose data-acquisition system was set up to carry out the experimental tests. All data were monitored with an Agilent 34972 A Data Acquisition Unit with three Agilent 34901 A 20 Channel Multiplexer Modules inserted. A specific measurement data spreadsheet using Benchlink Data Logger 3 was written and compiled for the system, supporting up to 66 inputs, with 16 bits A/D, 9600 bauds transmission speed and programmable gain for each individual channel. The sensors used during the experiment are shown in Fig. 3. The specifications of the measuring devices are presented in Table 2.

2.2. Experimental procedure

Before starting the tests, a calibration step of the measurement system was performed. In order to achieve accurate readings from the 18 thermocouples; it was necessary to calibrate them following a basic calibration process heating water in a thermo bath. Secondly, although the two PV modules were acquired as identical, a calibration process was done to be sure that the measurement of the power generated was the same for both modules. This step led to include a correction curve of the electrical power as a function of radiation to match both.

The experimental uncertainty, calculated according to ISO Guide

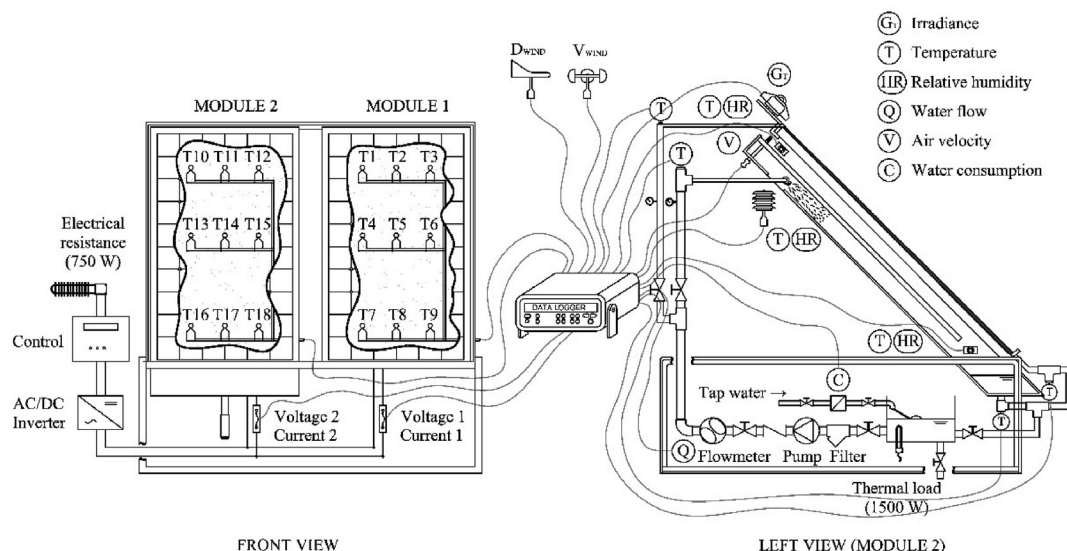


Fig. 3. Schematic diagram of the experimental prototype and measurement equipment.

Table 2
Measuring equipment used in the experimental prototype and measurement accuracy.

Measurement	Brand - Model	Measuring device	Measuring range	Accuracy
Ambient air temperature	E + E Elektronik (EE 21)	Capacitive sensor	−20 - 80°C	±0.3°C
Ambient Air relative humidity	E + E Elektronik (EE 21)	Capacitive sensor	0–100%	±2%
Air temperature	E + E Elektronik (EE 21)	Capacitive sensor	0–100°C	±0.4°C
Air relative humidity	E + E Elektronik (EE 21)	Capacitive sensor	0–100%	±2.5%
Wind direction	Young (05103L)	Balanced vane	0–360°	±3°
Wind Speed	Young (05103L)	4-blade helicoid propeller	0–50 m/s	±2.5m/s
Water temperature	Desin (ST-FFH Pt100)	4 wires Pt100/RTD	−200–600°C	±0.05°C
Module temperature	RS	K-Type thermocouple	−5–1100°C	±1.5°C
Irradiance	Kipp&Zonen CM-6B	First class pyranometer	0–1400 W/m ²	±1% RD
Water consumption	SENSUS MS8100	Volumetric water meter	0–500 l	±1% RD
Water flow rate	Kronhe Optiflux 1000	Electromagnetic flowmeter	0–2.5 m ³ /h	±0.3% RD
Air velocity	E + E (EE65)	Hot film anemometer	0–10 m/s	± (0.2 m/s+3% RD)

[6], with a level of confidence of 95% and using sensor specifications shown in Table 2, showed a value of 6.39% and 2.53% for the averaged efficiency and cooling power, respectively. Electrical measurements are very accurate. Specifically, the current is measured by using a shunt resistor (class 0.5), while the voltage is directly measured by the acquisition data system with an accuracy of ±5.1 mV. This translates into an uncertainty in the power output measurements lower than 1% and in the calculated percentage electric efficiency increase lower than 1.5%.

4 sets of experiments were performed throughout 2016–2017, both in summer and winter conditions according to Table 3. These tests were conducted with a thermal load (1.5 kW) and the combination of sprayed and slided water flowrates, shown in Table 3, in different ambient conditions.

The experimental procedure starts initiating the circulation of the water flow in both the nozzles and the drippers. The next step is switching on the electrical heaters (1.5 kW). In order to achieve steady operating conditions for all the variables, including temperatures, a startup period of 30 min was considered. From that moment, the prototype was working from early morning until late afternoon. UNE-EN 12975-2 Thermal solar systems and components - Solar collectors - Part 2: Test methods and Standard UNE 13741 "Thermal performance acceptance testing of mechanical draught series wet cooling towers" were selected as reference to define stationary conditions. For a test to be valid, variations in the test conditions shall be within the following limits during a 10 min period. The variations of the circulating water flow rate shall not be greater than 5%. The maximum deviation of the wet-bulb temperature may not exceed its average value during the test period (±1.5°C). The same is valid for the dry-bulb temperature with a deviation of (±4.5°C) and water temperatures (±1.5°C). The wind velocity shall not exceed 7 m/s for 1 min and its average value during the test period shall not exceed 3.5 m/s. Global solar irradiance was over 700 W/m² and deviation from the mean less than (±50 W/m²).

3. Results and discussion

To limit the length of the article, in this section we only describe the results of the test with 500 l/h in nozzles and 250 l/h in drippers

Table 3
Water flowrates tested.

Test	Nozzles flowrate (l/h)	Drippers flowrate (l/h)
1	250	0
2	500	0
3	500	50
4	500	250

performed on July 26, 2016. The main results of the other tests are summarized in the conclusions section. Module 1 (P1) will be the reference panel and Module 2 (P2) will be the one equipped with the chimney. The graphs in this section show the measurements averaged every 10 min. The areas shown in light green indicate the intervals that meet the stationarity conditions described in Section 2. Firstly, Figs. 4 and 5 briefly show the environmental conditions to which the test was performed. We select this day for having a completely clear sky as can be deduced from the evolution of solar irradiance. In addition, the presence of a wind level above 3 m/s allowed to discuss its influence on the results.

Fig. 6 shows the evolution of temperature and relative humidity of the air at the entrance of the chimney (IN), at the intermediate point (INT) and at the outlet (OUT). Observing the evolution of the temperature it is possible to verify how the air is cooled in the order of 5°C in the section called the evaporative zone (IN-INT) in which the water is atomized inside the chimney. In the ascending section on the rear face of the panel, in the area known as convective (INT-OUT), the air undergoes a slight cooling of only a few tenths of °C. This unexpected effect, since initially air heating was anticipated in this section, is justified because the panel is cooled by the sliding of water on its upper face.

As a low-scale cooling tower, the Evaporative Chimney cools water by a combination of heat and mass transfer. Baker and Shryock [2] developed a widely used cooling tower theory. They considered a cooling tower having one square foot of plan area; cooling volume V_T , containing extended water surface per unit volume A_V ; and water mass flow rate \dot{m}_w and air mass flow rate \dot{m}_a . The water is surrounded by the air and the interface is assumed to be a film of saturated air with an intermediate temperature at the

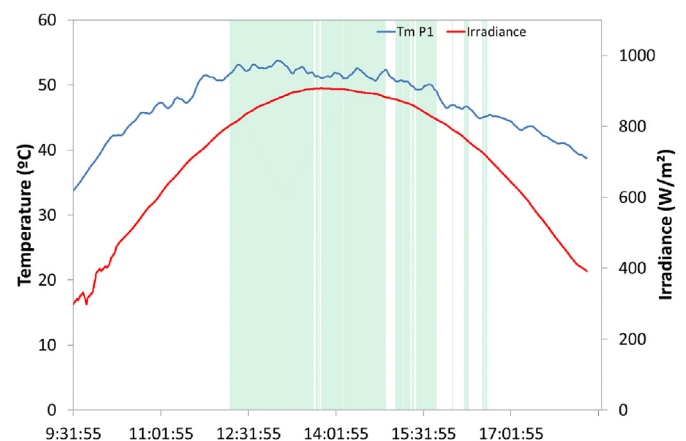


Fig. 4. Solar irradiance (26/07/2016) and Module 1 Temperature.

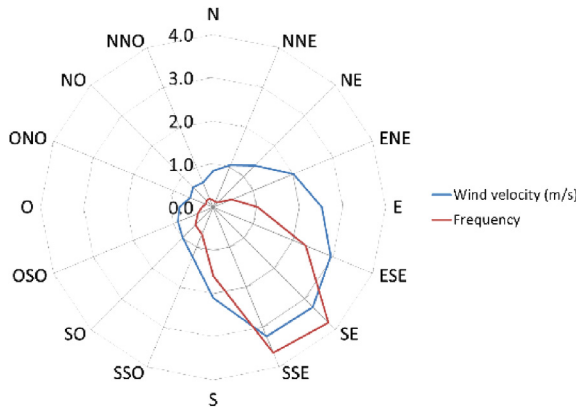


Fig. 5. Wind rose (26/07/2016).

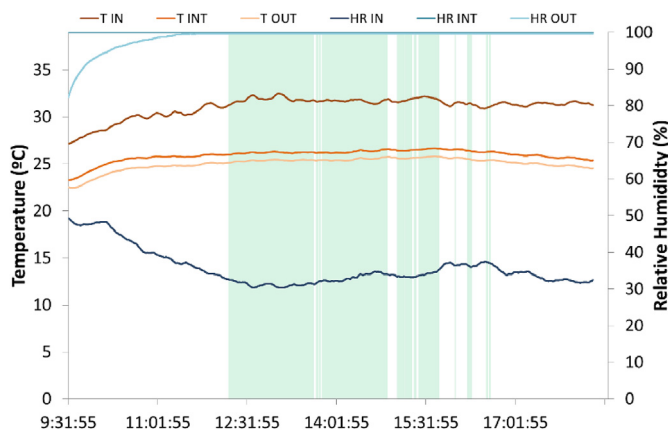


Fig. 6. Air temperature and relative humidity (inlet, intermediate and outlet).

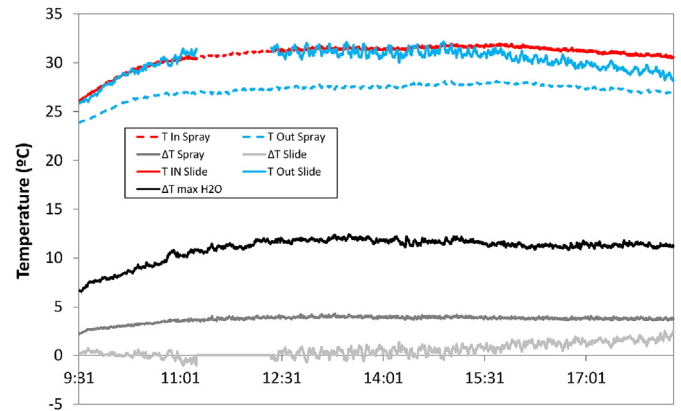


Fig. 7. Sprayed and slid water temperatures.

water temperature. Thus, the transfer from the interface to the airstream is proportional to the average enthalpy potential ($h_{s,w} - h$). Assuming a set of simplifying hypotheses, the steady-state energy and mass balances on an incremental volumen is:

$$-\dot{m}_w dh_{f,w} = \dot{m}_a dh_a = h_D A_V V_T (h_{s,w} - h) \quad (1)$$

From the Merkel model [5], water temperature decrease depends mainly on the incoming air wet-bulb temperature. The system's thermal efficiency (η_T) can be defined as the relation between actual water temperature reduction, the one existing between sprayed and drained water, $T_{w1} - T_{w2}$, and the water temperature's maximum difference, taking the ambient wet-bulb temperature as the physical limit to the drained water temperature, so:

$$\eta_T = \frac{T_{w1} - T_{w2}}{T_{w1} - T_{wb}} \quad (2)$$

Fig. 7 shows the evolution of the temperature in the two water currents. On the one hand, the graph shows the values of the temperatures in the evaporative section identified as sprayed water. On the other hand, the temperatures of the water that slides on the upper face of the panel are also represented. In view of the sprayed water, there is an average cooling throughout the day $\Delta T_{Spray} = T_{IN_{Spray}} - T_{OUT_{Spray}}$, of 3.7°C. A maximum water temperature difference, $\Delta T_{max} = T_{IN_{Spray}} - T_{wb}$, between 6.8°C and 12.1°C is measured, defined as the difference between the inlet temperature and the wet bulb temperature (between 19.3°C and 20.7°C for that day). The evaporative cooling efficiency is obtained by dividing

both values and an average value of 33.9% is obtained. The evolution of the water temperature that slides on the upper face of the PV panel, $\Delta T_{Slide} = T_{IN_{Slide}} - T_{OUT_{Slide}}$, is a very interesting discussion from a heat transfer point of view since there are times of the day when the water is heated (up to 0.6°C) and other times of day when the water cools down to 2.4°C. Particularly striking is the cooling suffered by the current at certain times of the day since even cooling the module the water comes out colder. This is justified because as the water slides simultaneously receives energy by convective heat transfer from the panel and gives heat to the environment by evaporation. As can be seen in the figure, the cooling is accentuated in the late afternoon when the panel is not so hot and there are higher levels of wind which improves the water evaporation.

Figs. 8 and 9 show the evolution of panel temperatures divided into three sections to show if stratification exists. Fig. 8 shows, as an example, a test in which only water atomization is carried out and it can be seen how the temperature of the stack module (P2) is lower than the module unmodified essentially in the lower section. Observing the intermediate and upper temperatures, it can be seen that the temperatures of both panels increase. In the case of the sliding test shown in Fig. 9, two effects are clearly seen. On the one hand a greater cooling of the panel is achieved reaching differences of up to 20.2°C with an average value over the day of 15°C. On the other hand it is observed that the temperature of the module 2 is much more uniform.

Fig. 10 shows the rise of the module temperature ($T_m - T_{amb}$) with respect to the irradiance on the two modules installed in the

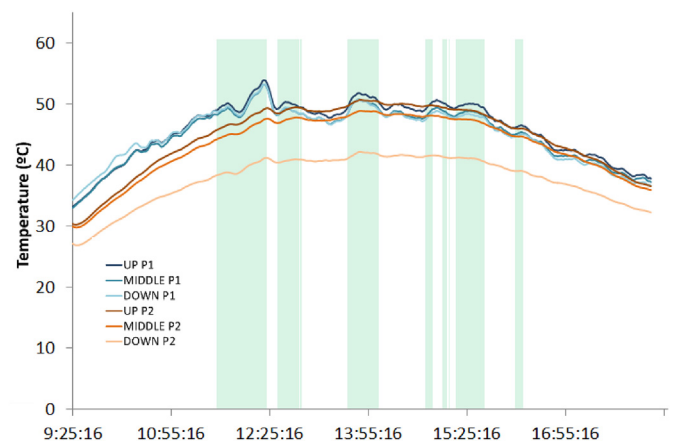


Fig. 8. Temperature of the panels by horizontal sections. Test without water slide.

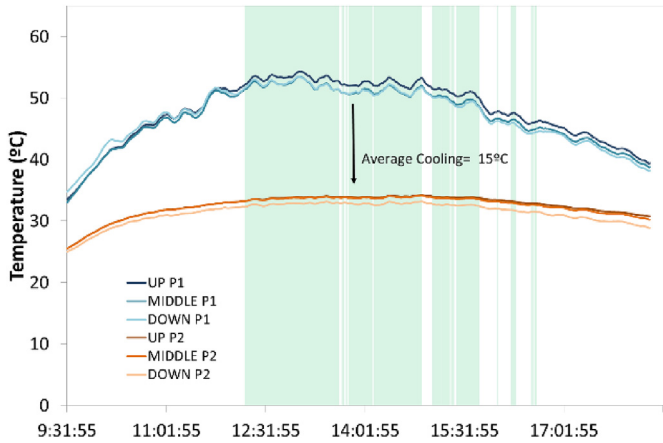


Fig. 9. Temperature of the panels by horizontal sections with water sliding.

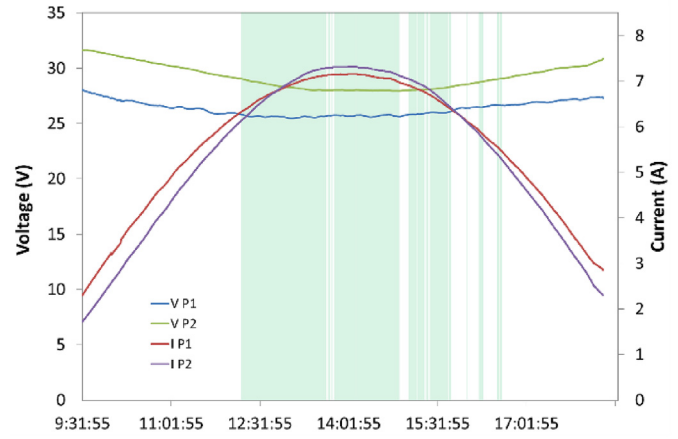


Fig. 11. PV panels Voltage and current.

pilot plant. In order to contextualize the results of our facility with those available in the literature, they are compared with the work of Nordmann and Clavadetscher [13]. The authors analyzed the effect of the elevated cell-temperature on the annual performance of PV systems of different mounting (freestanding, roof-mounted and integrated PV façades) from different geographic locations. As it can be seen, the results of Module 1 match with freestanding systems results which usually allow a free airflow around the modules as it might be expected. In addition, a comparison is included with the results of the work of Kaiser et al. [7]. They provided an open air channel beneath the module and study the influence of the air gap size and the forced convection induced by the building ventilation system on the cell temperature of a BIPV configuration. The results show that the temperature of the Module 2 are clearly below to that of a module with the maximum ventilation.

The electrical performance of the panels is now described. The voltage and current generated by the photovoltaic panels is shown in Fig. 11 and electrical power in Fig. 12. The latter starts to be greater in the standard panel because this can be due to the fact that the sliding water is hotter than the ambient temperature, this happens until 11:00 a.m. (civil time). In the central hours of the day improvements are achieved up to 17 W per panel which means a 9.75% improvement in performance.

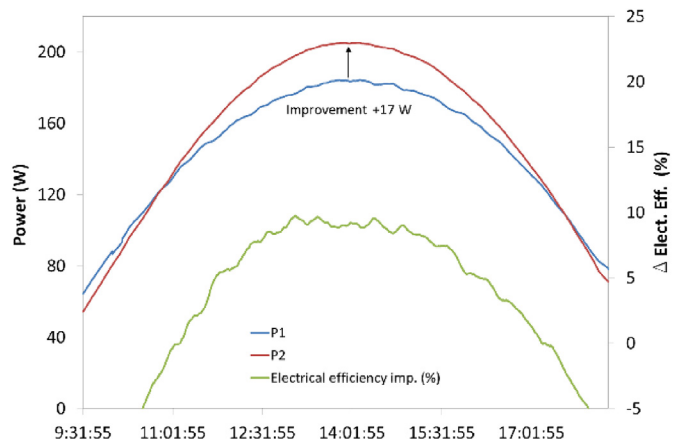


Fig. 12. Electrical power and Improvement (%).

Finally, Fig. 13 shows the relationship between the improvement obtained in the electrical efficiency and wind velocity. It can be observed that the improvement obtained in the module with chimney and sliding water is already independent of the wind level, showing a dependence with the difference between panel temperatures as expected.

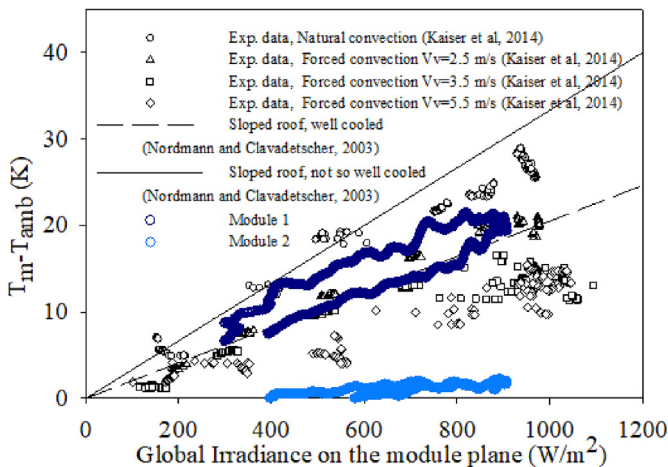


Fig. 10. Comparison of results obtained with those of the literature in terms of PV panel and ambient temperature difference vs. irradiance.

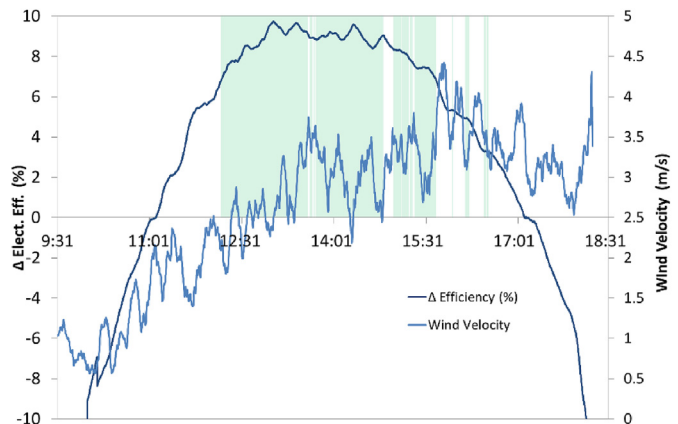


Fig. 13. Performance difference (P2–P1) vs. wind speed (m/s).

4. Conclusions

In the present work, several types of tests have been carried out in order to know the thermal and electrical performance of the evaporative photovoltaic solar chimney. A new hydraulic design has been made and built to allow water to slide over the chimney panel by means of drippers. The effect of sliding on the panel has also been analyzed as a starting point. From the first set of tests, with only 250 l/h in the nozzles, it was concluded that this flow rate will never be a suitable working point. The electrical efficiency of the panel with the chimney were practically always lower than the standard one in a value around 2%. This is justified since the air velocity inside the chimney is lower than the wind velocity. The second set of tests (500 l/h in the nozzles) were similar to those carried out in the summer of 2015 and which corroborated the conclusions obtained then. The third set of tests was what really marks the present work. Tests were carried out by sliding water above the panel maintaining 500 l/h in the nozzles. The conclusions is that, the higher flow rate supplied to the drippers, the better panel performance. The 50 l/h test showed an electrical efficiency improvement of 6–7%, while at 250 l/h it was maintained around 10%, with a peak of 11%. It was also observed that the wind no longer influences the electrical efficiency difference. Without sliding water above, the wind was a determining factor, as it ventilates the panel without chimney exceeding the ventilation induced by the chimney. With the new design, the wind helps to cool the sliding water and therefore the PV panel. Including the sliding water, what really determines the performance of the panel is the difference in temperature between panels, reaching 20°C and without any stratification on the whole panel. The next step will be a more accurate search of the combination of water flows leading to optimum system performance.

Acknowledgements

The authors acknowledge financial support from Spanish Ministry of Economy, Industry and Competitiveness, the State Research Agency (AEI) and the European Union by European Regional Development Fund – FEDER Project ENE2017-83729-C3-1-R.

The authors also wish to acknowledge the collaboration in the experimental work of the following Mechanical and Electrical Engineering students: S. Rodríguez, J.F. Bernal, P. Díez, H. Garcés, C. Selva, V. García, J. Navas, E. Gálvez and F. Martínez; and especially to E. Sánchez for his amazing work as a lab technician.

References

- [1] H. Bahaidarah, A. Subhan, P. Gandhidasan, S. Rehman, Performance evaluation of a pv (photovoltaic) module by back surface water cooling for hot climatic conditions, *Energy* 59 (C) (2013) 445–453. URL, <http://EconPapers.repec.org/RePEc:eee:energy:v:59:y:2013:i:c:p:445-453>.

- [2] D. Baker, H.A. Shryock, A comprehensive approach to the analysis of cooling tower performance, *J. Heat Tran.* 83 (3) (1961) 339–349. URL <http://heattransfer.asmedigitalcollection.asme.org/article.aspx?articleid=1432350>.
- [3] European-Commission, Horizon 2020 Work Programme 2016-17. 'secure, Clean and Efficient Energy', 2015. URL, <https://ec.europa.eu/programmes/horizon2020/en/h2020-section/secure-clean-and-efficient-energy>.
- [4] K. Fong, T. Chow, C. Lee, Z. Lin, L. Chan, Comparative study of different solar cooling systems for buildings in subtropical city, *Sol. Energy* 84 (2) (2010) 227–244. URL, <http://www.sciencedirect.com/science/article/pii/S038092X09002667>.
- [5] W. Haussler, K. Stadt, Merkel Theory of Evaporative Cooling, 1977.
- [6] ISO, Guide to the Expression of Uncertainty in Measurement (GUM)-Supplement 1: Numerical Methods for the Propagation of Distributions, International Organization for Standardization, Geneva, 2004. Vol. ISO draft guide DGUIDE99998.
- [7] A. Kaiser, B. Zamora, R. Mazón, J. García, F. Vera, Experimental study of cooling bipv modules by forced convection in the air channel, *Appl. Energy* 135 (2014) 88–97. URL, <http://www.sciencedirect.com/science/article/pii/S0306261914008903>.
- [8] M. Lucas, F. Aguilar, J. Ruiz, C. Cutillas, A. Kaiser, P. Vicente, Photovoltaic evaporative chimney as a new alternative to enhance solar cooling, *Renew. Energy* 111 (Supplement C) (2017a) 26–37. URL, <http://www.sciencedirect.com/science/article/pii/S0960148117302781>.
- [9] Lucas, M., Vicente, P., Ruiz, R., Aguilar, V., Garcia, C., Sanchez, K., Apr. 27 2017b. Photovoltaic evaporative chimney for simultaneous actuation and heat dissipation in an air conditioning system. WO Patent App. PCT/ES2016/070,740. URL <http://www.google.com.pg/patents/WO2017068220A1?cl=en>.
- [10] M. Mattei, G. Notton, C. Cristofari, M. Muselli, P. Poggi, Calculation of the polycrystalline {PV} module temperature using a simple method of energy balance, *Renew. Energy* 31 (4) (2006) 553–567. URL, <http://www.sciencedirect.com/science/article/pii/S096014810500073X>.
- [11] D. Mugnier, R. Fedrizzi, R. Thygesen, T. Selke, New generation solar cooling and heating systems with {IEA} {SHC} task 53: overview and first results, *Energy Procedia* 70 (2015) 470–473, international Conference on Solar Heating and Cooling for Buildings and Industry, {SHC} 2014. URL, <http://www.sciencedirect.com/science/article/pii/S1876610215002714>.
- [12] D. Neyer, M. Ostheimer, D. Mugnier, S. White, 10 key principles for successful solar air conditioning design - a compendium of ieas shc task 48 experiences, *Sol. Energy* 172 (Part 1) (15 September 2018) 78–89, <https://doi.org/10.1016/j.solener.2018.03.086>.
- [13] T. Nordmann, L. Clavadetscher, Understanding temperature effects on pv system performance, in: *Photovoltaic Energy Conversion, 2003. Proceedings of 3rd World Conference on*, vol. 3, IEEE, 2003, pp. 2243–2246.
- [14] S. Odeh, M. Behnia, Improving photovoltaic module efficiency using water cooling, *Heat Tran. Eng.* 30 (6) (2009) 499–505. URL, <https://doi.org/10.1080/01457630802529214>.
- [15] S.R. Reddy, M.A. Ebadian, C.-X. Lin, A review of pvt systems: thermal management and efficiency with single phase cooling, *Int. J. Heat Mass Tran.* 91 (2015) 861–871. URL, <http://www.sciencedirect.com/science/article/pii/S0017931015304002>.
- [16] C. Schwingshackl, M. Petitta, J. Wagner, G. Belluardo, D. Moser, M. Castelli, M. Zebisch, A. Tetzlaff, Wind effect on {PV} module temperature: analysis of different techniques for an accurate estimation, *Energy Procedia* 40 (2013) 77–86. URL, <http://www.sciencedirect.com/science/article/pii/S1876610213016044>.
- [17] H. Teo, P. Lee, M. Hawlader, An active cooling system for photovoltaic modules, *Appl. Energy* 90 (1) (2012) 309–315, energy Solutions for a Sustainable World, Special Issue of International Conference of Applied Energy, ICA2010, April 21–23, 2010, Singapore. URL, <http://www.sciencedirect.com/science/article/pii/S0306261911000201>.
- [18] F. Yik, J. Burnett, I. Prescott, Predicting air-conditioning energy consumption of a group of buildings using different heat rejection methods, *Energy Build.* 33 (2) (2001) 151–166. URL, <http://www.sciencedirect.com/science/article/pii/S0378778800000943>.